Pergamon

Phys. Chem. Earth (C), Vol. 26, No. 1-3, pp. 97–106, 2001

1464-1917/00/$ - see front matter

PII: S1464-1917(00)00095-7

Comparison of Solitary Waves and Wave Packets Observed at Plasma Sheet Boundary to Results from the Auroral Zone

C. Cattell[1], J. Dombeck[1], A. Keiling[1], J. Wygant[1], R. Bergmann[2], M. K. Hudson[3], C. Kletzing[4], F. S. Mozer[5], M. Temerin[5], I. Roth[5] and G. Parks[6]

[1]School of Physics and Astronomy, University of Minnesota, Minneapolis, MN, USA
[2]Eastern Illinois University
[3]Dept. of Physics and Astronomy, Dartmouth College, Hanover, NH
[4]Dept. of Physics and Astronomy, University of Iowa, Iowa City, IA, USA
[5]Space Sciences Laboratory, University of California, Berkeley, CA, USA
[6]Geophysics Program, University of Washington, Seattle, WA, USA

Received 22 November 1999; revised 19 may 2000; accepted 30 June 2000

Abstract. The plasma sheet boundary, at distances intermediate between the auroral acceleration region and the regions where energy conversion associated with substorms occurs, is very dynamic with electron and ion beams, field-aligned currents and many types of waves and non-linear structures. We discuss electric and magnetic fields observations of waves occurring at two very different time-scales. At the longer scales (10's of seconds), Wygant et al. (2000) have shown that the observed fields are associated with Alfvenic fluctuations which have their largest electric field normal to the average plane of the plasma sheet (δE_N). The simultaneously observed magnetic field perturbations are azimuthal(δB_T), resulting in a Poynting flux along the geomagnetic field. The observations are consistent with an incompressible, transverse electromagnetic surface shear Alfven mode at the surface of the plasma sheet boundary. The local $\delta E_N/\delta B_T$ is consistent with V_A. The waves provide an intense earthward Poynting flux sufficient to provide the energy necessary for the energization of auroral electron beams. In addition, the large amplitude surface waves are magnetically conjugate (to within 1 degree) to intense auroral emission as determined from the UVI imager, whereas weak aurora are correlated with small amplitude electric fields. Particle detectors simultaneously observe ions flowing up the field line away from the earth, providing further evidence that low altitude acceleration is occurring on conjugate magnetic field lines. At small scales, large amplitude solitary waves are frequently observed, and ion acoustic, lower hybrid, and Langmuir wave packets are sometimes seen. There are clear differences between the solitary wave observations at the plasma sheet boundary and in the low altitude auroral zone. At high altitudes, only electron mode solitary waves have been identified and they occur both in regions of upward and downward field-aligned current, in contrast to the auroral zone where ion solitary waves occur in upward currents and electron solitary waves occur primarily in downward currents. This difference may because the growth of ion acoustic solitons requires that the plasma be strongly magnetized ($f_{ce}/f_{pe} >> 1$) which is not the case for the observed high altitude plasma sheet boundary crossings. The high altitude events are associated with a wide variety of electron distribution types, whereas the low altitude events occur in regions of flat-top electron beam distributions. Preliminary evidence suggests that the high altitude events may be BGK electron holes, as has been shown for the low altitude events. For the parameter regime usually observed at high altitudes, electron holes would be stable. In addition, initial work on electron acoustic solitons suggests that these compressive waves would occur only for a limited range of parameters, so they are unlikely to explain the high altitude solitary waves.

Correspondence to: Cynthia Cattell

1 Introduction

The plasma sheet boundary is a very dynamic region which often contains ion and electron beams, field-aligned currents, spiky electric fields and strong waves. It is generally thought to be on magnetic field lines that map to the poleward boundary of the night-side auroral zone, as well as to the more distant portions of the geomagnetic tail where energy conversion processes associated with reconnection occur.

Understanding the wave processes which occur at intermediate radial distances (~4-7 Re) on the plasma sheet boundary is important for understanding auroral acceleration and its relationship to the dynamics of the plasma sheet. In this paper, we describe observations of a variety of waves observed in time domain electric and magnetic field data obtained by the Polar satellite. We will focus on waves observed at two very different time scales - solitary waves and Langmuir wave packets at millisecond time scales (Cattell et al., 1998; 1999), and Alfven waves with time scales of 10's of seconds (Wygant et al., 1999; Keiling et al., 1999).

The observations at high altitudes on the plasma sheet boundary will be compared to low altitude, auroral zone measurements made by Polar and FAST. Similarities and differences between measurements of solitary waves by Polar, at the plasma sheet boundary, and FAST, in the auroral zone will be used to elucidate wave generation mechanisms and dynamic effects. The observations were made in very diverse plasma regimes which allows us to examine a number of parameters including f_{ce}/f_{pe} from ~0.1 to >10, Te/Ti, a broad range of plasma density and composition, as well as the presence or absence of cold particles and of various possible free energy sources including ion beams, electron beams and field-aligned currents. We will discuss whether the observations are consistent with the occurrence of two of the basic types of solitary waves (ion acoustic and electron acoustic), in addition to BGK electron holes, and provide constraints on possible generation mechanisms. The correlation between large amplitude Alfven waves at high altitudes and the energy flux associated with auroral electron beams, as inferred from the UVI instrument, will also be addressed in order to understand the processes which power auroral acceleration.

The data sets used in the study are described in Section 2. Observations of large amplitude Alfven waves, the associated Poynting flux and auroral images are discussed in Section 3. Solitary waves and Langmuir packets are addressed in Section 4. Section 5 presents our conclusions and ongoing studies.

2 Data Sets

The data for this study were obtained as the Polar satellite crossed the plasma sheet boundary at radial distances of ~4 - 7 Rc at magnetic local times of ~20 – 02. The electric field and spacecraft potential measurements were made by the double probe electric field instrument (EFI) on the Polar satellite (Harvey et al., 1995). The spacecraft potential is indicative of thermal electron density (Pedersen, 1995). EFI obtains 3d measurements of the electric field at 20 samples/second and, in addition, obtains bursts (waveform capture) of high time resolution data in many different modes. Electric field data sampled at 8000 samples/s are utilized herein. In addition to the electric field (potential difference between opposing probes), the delay time between signals at opposing probes were examined to estimate the propagation speed of electric field structures (see Cattell et al., 1999). Electric field data were rotated into a magnetic field-aligned coordinate system and the parallel component was examined for candidate solitary waves. Timing analysis was limited to events where one of the two spin plane boom pairs is nearly aligned along the magnetic field. In these cases, the signal from each single probe was splined to provide an identical time basis for all signals and spacecraft potential variations were removed using the perpendicular boom pair. The time delay between the observation of the solitary wave signal at opposing probes was determined using a cross correlation analysis. Coupled with the projected probe separation along the magnetic field, the time delay was used to estimate the propagation velocity of the solitary waves. Details of this procedure will be described elsewhere (Dombeck et al., manuscript in preparation). AC magnetic field data were obtained from the search coils (Gurnett et al., 1995) which were sampled in the burst memory at the same rate as the electric field. DC magnetic field data were obtained from the fluxgate magnetometers (Russell et al., 1995). Plasma data from the Hydra instrument (Scudder et al., 1995) and images from UVI (Torr et al., 1995) are also utilized.

3 Alfven waves and the associated Poynting flux on the plasma sheet boundary

Wygant et al. (2000) have discussed the relationship between Alfvenic fluctuations on the plasma sheet boundary and intense aurora as observed by the UVI imager on Polar. Figure 1a (from Wygant et al., 2000) presents 6 second averaged electric and magnetic field data and 13.8 second averaged plasma measurements on May 9, 1997 as Polar moved from the lobe to the plasma sheet from L=9.4 to 4.8 near 22 MLT. The top panel of Fig. 1 shows the z GSE (northward) component of the electric field , approximately perpendicular to the average plane of the plasma sheet; the second panel displays the y (eastward) component of the magnetic field with a Tsyganenko model magnetic field subtracted; and the third panel displays the Poynting flux along the ambient average magnetic field, calculated from the three components of the perturbation electric field and three components of the perturbation magnetic field. These perturbation fields were calculated by detrending each component of the field by subtracting a 180 second running average from the original data. The Poynting flux vector was then projected along the average magnetic field direction calculated from the measured magnetic field vector averaged over 180 seconds. The fourth panel shows the sum of the electron and ion energy flux along the magnetic field (positive is downward) calculated from the Hydra measurements. The fifth panel shows the electron density. The bottom two panels present color coded energy-time spectrograms of ion and electron energy fluxes. The vertical brackets in the top panel delineate time periods when the

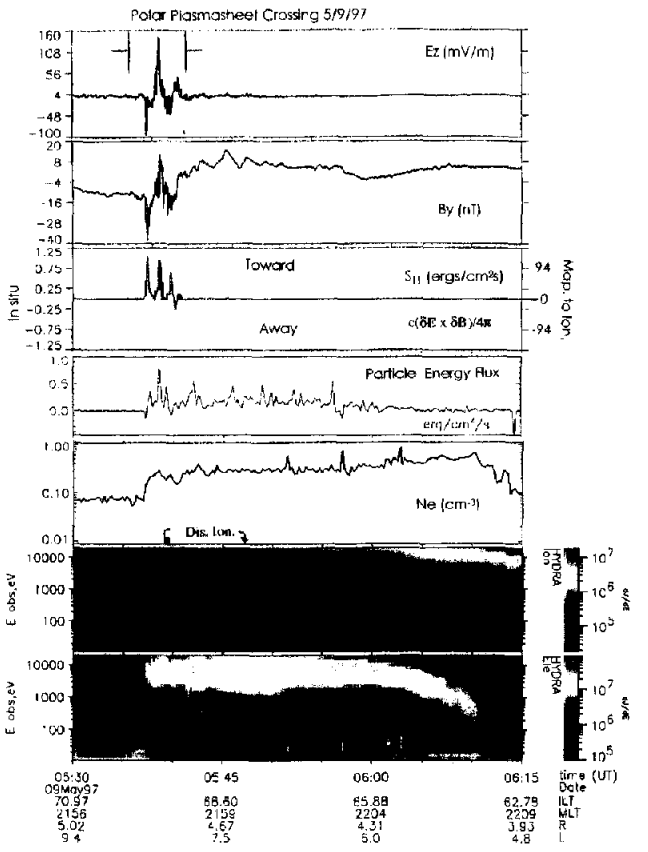

Figure 1a. Measurements from Polar spacecraft crossing of the PSBL on 5/9/1997. The panels show (from top to bottom) the electron density, the component of electric field approximately normal to the plane of the plasma sheet, the magnetic field (model subtracted) perpendicular to the local magnetic field in the plane of the plasma sheet and the Poynting flux component along the magnetic field. The fourth panel is the total particle energy flux along the magnetic field with positive values corresponding to earthward flux. The fifth panel is the electron density obtained from the Hydra measurements. The two lower two panels display Hydra energy flux-time spectrograms of electrons and ions.

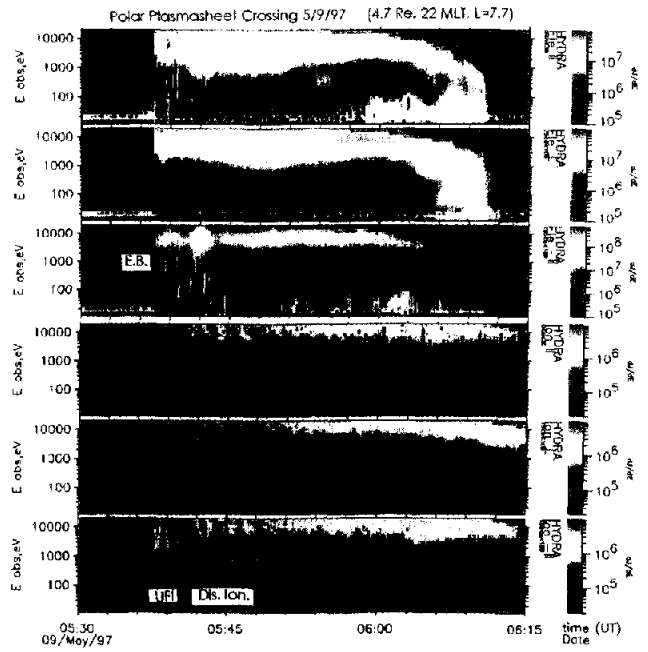

Figure 1b. Hydra electron and ion energy fluxes sorted into pitch angle bins

foot of the spacecraft magnetic field line mapped to within one degree of the regions of intense (>16 ergs/cm^{2}s) auroral emission determined from the UVI images shown in Fig. 2. The particle data show that Polar entered the plasma sheet boundary at 5:37 UT at a geocentric distance of about 4.9 Re. The entry into the plasma sheet is most clearly indicated by the order of magnitude increases in the 2-20 keV electrons. The electric field enhancements are located on the high density side of a jump in density from about 0.1 cm^{-3} on the lobe side to 0.4 cm^{-3} on the plasma sheet side.

The electric field data show a series of three fluctuations ranging between -100 mV/m and 140 mV/m. This five minute time interval coincides with the passage of the spacecraft through an upward current sheet as indicated by a shift in the dc level of By. Superimposed on this shift are three ~20 nT fluctuations in the magnetic field. These transverse magnetic field fluctuations are similar in wave form to those in the electric field. The total magnitude of the magnetic field (not shown) has fluctuations on the order of 1 nT over similar time scales during these waves. Thus the transverse variations in the magnetic field strongly dominate over the compressional variations. The net Poynting flux calculated from the detrended electric and magnetic fields consists of contributions from Alfven waves propagating towards and away from the earth along the background magnetic field. The fact that the Poynting flux is directed towards the earth indicates that the energy flux due the Alfven waves propagating towards the earth is larger than that from waves propagating away from the earth. The existence of waves propagating away from the earth can be deduced from the observed phase differences between the electric and magnetic fields, as will be discussed later. The net Alfven wave power for this crossing is directed towards the earth with amplitudes ranging up to 0.6 to 1 ergs/cm^{2}s. The scale on the right side of the Poynting flux plot, which gives the magnitude as mapped to 100 km altitude, shows that the mapped Poynting flux has values from ~ 24 to 100 ergs/cm^{2}s. This mapped Poynting flux is much larger than the Poynting flux previously measured in situ at lower altitudes in (or below) the auroral acceleration region, which suggests that a significant portion of this energy flux is being dissipated through particle acceleration before it reaches the ionosphere.

Figure 1b presents the electron and ion energy flux as a function of energy for pitch angles between 0 and 30 degrees, 75 and 105 degrees, and 150 to 180 degrees. The data show that the electric field structures and earthward Poynting flux coincide almost exactly with 1-10 keV up-going ions (labeled "UFI") which have been accelerated at lower altitudes in the acceleration region. They are located at the outer boundary of the plasma sheet and last for about 3 minutes. These ions are almost completely field aligned, providing evidence that the Polar spacecraft is magnetically conjugate to the auroral acceleration region. There is also evidence for field-aligned electron beams traveling both towards and away from the Northern Hemisphere's ionosphere. The electron beams, visible in the first and third panels of Fig. 1b, occur during the interval labeled "E.B.".

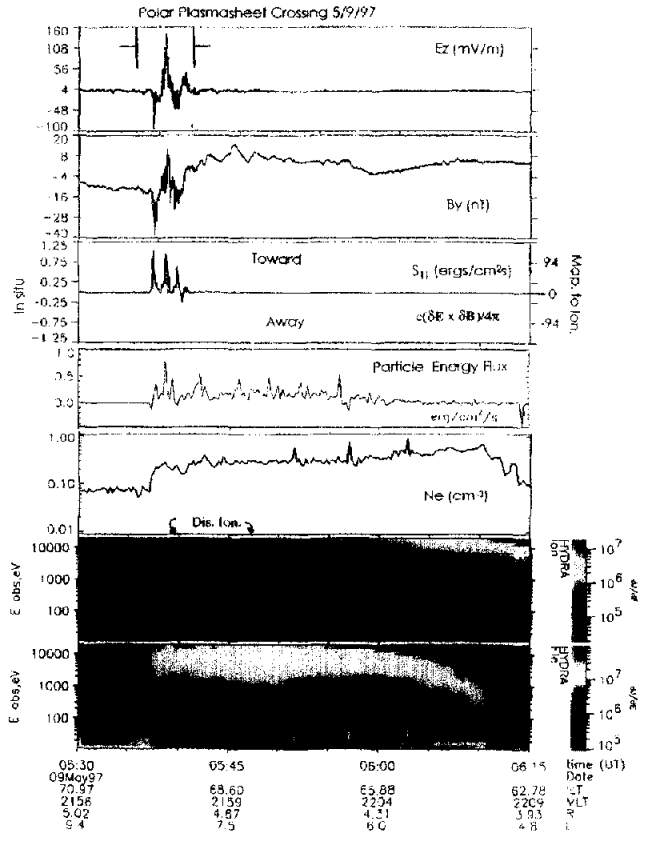

Figure 1a. Measurements from Polar spacecraft crossing of the PSBL on 5/9/1997. The panels show (from top to bottom) the electron density, the component of electric field approximately normal to the plane of the plasma sheet, the magnetic field (model subtracted) perpendicular to the local magnetic field in the plane of the plasma sheet and the Poynting flux component along the magnetic field. The fourth panel is the total particle energy flux along the magnetic field with positive values corresponding to earthward flux. The fifth panel is the electron density obtained from the Hydra measurements. The two lower two panels display Hydra energy flux-time spectrograms of electrons and ions.

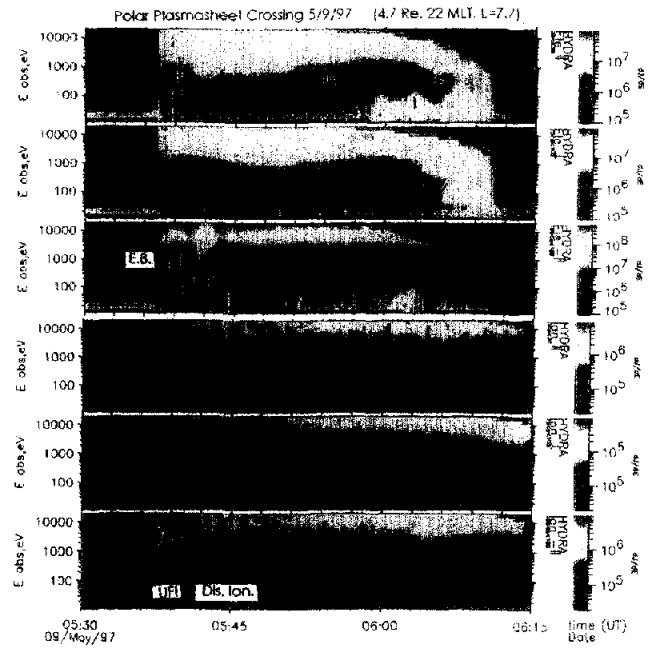

Figure 1b. Hydra electron and ion energy fluxes sorted into pitch angle bins

foot of the spacecraft magnetic field line mapped to within one degree of the regions of intense (>16 ergs/cm^{2}s) auroral emission determined from the UVI images shown in Fig. 2. The particle data show that Polar entered the plasma sheet boundary at 5:37 UT at a geocentric distance of about 4.9 Re. The entry into the plasma sheet is most clearly indicated by the order of magnitude increases in the 2-20 keV electrons. The electric field enhancements are located on the high density side of a jump in density from about 0.1 cm^{-3} on the lobe side to 0.4 cm^{-3} on the plasma sheet side.

The electric field data show a series of three fluctuations ranging between -100 mV/m and 140 mV/m. This five minute time interval coincides with the passage of the spacecraft through an upward current sheet as indicated by a shift in the dc level of By. Superimposed on this shift are three ~20 nT fluctuations in the magnetic field. These transverse magnetic field fluctuations are similar in wave form to those in the electric field. The total magnitude of the magnetic field (not shown) has fluctuations on the order of 1 nT over similar time scales during these waves. Thus the transverse variations in the magnetic field strongly dominate over the compressional variations. The net Poynting flux calculated from the detrended electric and magnetic fields consists of contributions from Alfven waves propagating towards and away from the earth along the background magnetic field. The fact that the Poynting flux is directed towards the earth indicates that the energy flux due the Alfven waves propagating towards the earth is larger than that from waves propagating away from the earth. The existence of waves propagating away from the earth can be deduced from the observed phase differences between the electric and magnetic fields, as will be discussed later. The net Alfven wave power for this crossing is directed towards the earth with amplitudes ranging up to 0.6 to 1 ergs/cm^{2}s. The scale on the right side of the Poynting flux plot, which gives the magnitude as mapped to 100 km altitude, shows that the mapped Poynting flux has values from ~ 24 to 100 ergs/cm^{2}s. This mapped Poynting flux is much larger than the Poynting flux previously measured in situ at lower altitudes in (or below) the auroral acceleration region, which suggests that a significant portion of this energy flux is being dissipated through particle acceleration before it reaches the ionosphere.

Figure 1b presents the electron and ion energy flux as a function of energy for pitch angles between 0 and 30 degrees, 75 and 105 degrees, and 150 to 180 degrees. The data show that the electric field structures and earthward Poynting flux coincide almost exactly with 1-10 keV up-going ions (labeled "UFI") which have been accelerated at lower altitudes in the acceleration region. They are located at the outer boundary of the plasma sheet and last for about 3 minutes. These ions are almost completely field aligned, providing evidence that the Polar spacecraft is magnetically conjugate to the auroral acceleration region. There is also evidence for field-aligned electron beams traveling both towards and away from the Northern Hemisphere's ionosphere. The electron beams, visible in the first and third panels of Fig. 1b, occur during the interval labeled "E.B.".

brightest auroral emission features. The peak values of the Poynting flux are up to a factor of 3 larger than the energy flux due to precipitating electrons as estimated by the imager. The mapped Poynting flux is about 100 ergs/cm^{2}s, while the energy flux associated with the region of bright auroral emission is typically 20 ergs/cm^{2}s in the region conjugate to the spacecraft position. The incident Poynting flux must account not only for the energy flux of precipitating electrons, but also for ionospheric Joule heating, and ion acceleration. In addition, the spatial/temporal scales over which the Poynting flux varies are much smaller than those resolved by the images. The images average over ionospheric spatial scales of about 0.5 degrees. This is much larger than the 0.1 to 50 km spatial scales of discrete auroral arcs. Under these circumstances, the peak value of the Poynting flux measured by the higher resolution satellite measurements should be an order of magnitude larger than the value of the electron energy flux inferred from the averaged images. The comparison of the Poynting flux measurements at high altitude to the UVI images suggests that the Poynting flux is in part being converted to particle energy in the acceleration region-probably by parallel fields associated with the several hundred mV/m to one V/m localized perpendicular electric field structures first observed by the S3-3 spacecraft over twenty years ago and now resolved routinely by the Polar and FAST spacecraft.

These observations are strong evidence that the Poynting flux due to Alfven waves is responsible for powering the acceleration of auroral electron beams and is a major mechanism for transporting energy from the tail to the ionosphere. These observations further suggest that Poynting flux through the radiation of large amplitude Alfven waves may be a significant energy sink for energy release processes in the tail such as reconnection since in our examples, at Polar altitudes, the Poynting flux was comparable or larger than the total energy flux due to electrons and ions. The geometry of these electric and magnetic field fluctuations is sometimes similar to the shear mode Alfven surface waves first proposed by Hasegawa (1976) as a mechanism for powering the aurora. Wygant et al. (2000) and Keiling et al. (2000) present more examples of such conjunctions and a more detailed discussion of the observations and interpretation, as well as relevant theoretical models.

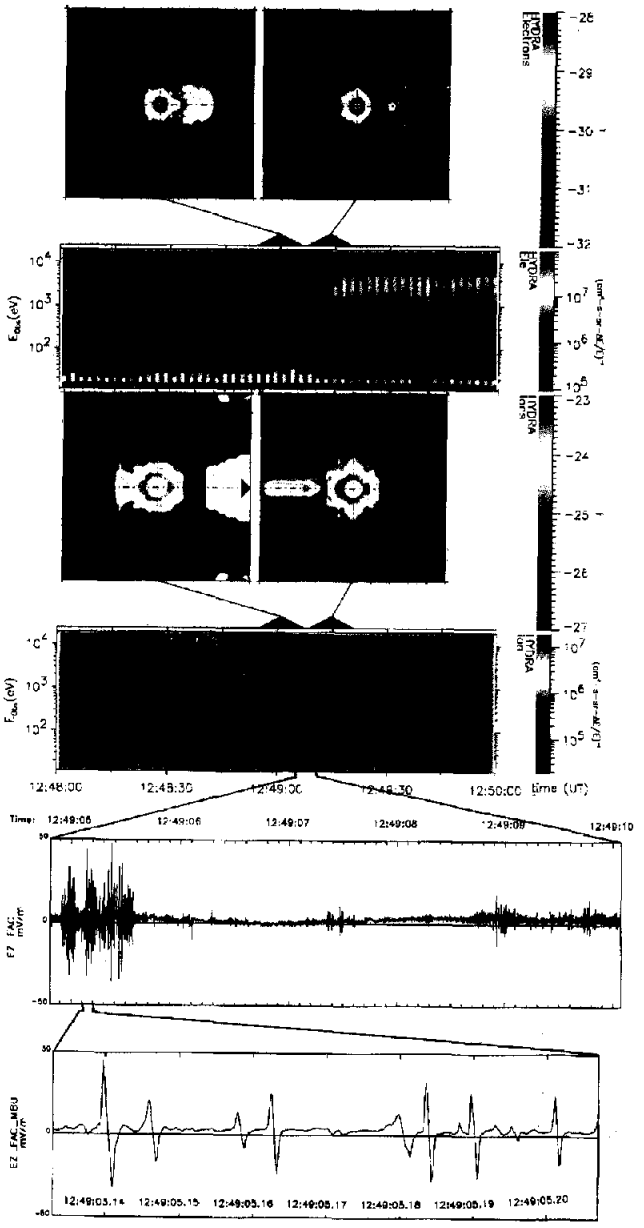

Figure 3. Plasma and electric and magnetic field data for plasma sheet boundary crossing on May 5, 1997. From top to bottom the panels show electron distribution function for two intervals at the burst time, the electron energy time spectrogram, two ion distribution functions, the ion energy-time spectrogram, the east-west component of the magnetic field (indicative of filed-aligned currents), and the field-aligned component of the electric field for the burst.

4 Solitary waves

One type of structure, observed in electric field waveform data, which has received much study is solitary waves. Solitary waves, which were interpreted as negative potential pulses traveling up the magnetic field, were first observed in the auroral zone (Temerin et al., 1982, Bostrom et al., 1988). These solitary waves, which occur in association with ion beams propagating away from the ionosphere, have been associated with the ion acoustic mode and have been identified as ion holes. Later, lower amplitude solitary structures, interpreted as electron holes, were identified in the distant plasma sheet (Matsumoto et al., 1994). Utilizing data from the FAST spacecraft, Ergun et al. (1998) have identified a new type of solitary wave, associated with cold electron beams, which propagates in the beam direction at ~4500 km/s. These waves have an electromagnetic signature and are interpreted as electron holes traveling with the beam. Similar structures in the low altitude Polar data were described by Mozer et al. (1997) and Bounds et al. (1999). Preliminary results from Polar have also provided evidence for similar fast moving solitary waves at high altitudes

(Cattell et al., 1998; 1999; Franz et al, 1998). Observations by Wind at the bow shock (Bale et al, 1999) have also identified large amplitude solitary structures interpreted as electron holes. In addition, Dubouloz et al. (1991) postulated that negative potential electron acoustic solitary waves were the source of the broadband electrostatic noise observed in the low altitude dayside auroral zone. These and many other similar observations indicate that solitary waves are ubiquitous in naturally occurring plasmas.

Theoretical work on solitary waves initially focussed on ion acoustic solitons, which, for a simple system with one ion and one electron species, were shown to be compressive (positive potential) structures propagating slightly faster than the ion acoustic speed. Such solitons have not yet been observed; the observed ion solitons are rarefractive. Many more complex, multi-component systems have been studied, analytically, numerically and via simulations, providing information of propagation velocities, growth and stability, and structure (compressive or rarefractive) in various regions of parameter space. Similar studies made of electron acoustic solitary waves, indicate that, for most plasma models, the structures are negative potential and propagate above the electron acoustic speed. Positive potential structures occur only in a very restricted parameter space. The most common theoretical explanation for the fast moving solitary waves is an electron hole mode, such as analytic BGK modes (Muschietti et al., 1999) or evolution of a bump on tail instability or electron two stream instability (Omura et al., 1996; Mottez et al., 1997; Matsumoto et al., 1999; Goldman et al., 1999; and references therein).

The plasma sheet boundary crossing shown in Fig. 3 occurred on May 5, 1997 at a radial distance of 5.3 Re and at 22 MLT, in a region of upward field-aligned current. The top panel shows 2 electron distribution functions, the second panel shows the electron energy spectrum, the third panel shows the ion distributions, the fourth panel presents the ion energy spectrum, and the fifth panel plots the component of the electric field parallel to the geomagnetic field for the 6s burst. The observations are similar to those which are seen in low altitude auroral zone upward current sheets in that there are upgoing ion beams, as well as downgoing electron beams (peaked at a velocity of ~10,000 km/s) and a clear upgoing electron loss cone signature in the electron distributions. The solitary waves had parallel electric fields up to~80 mV/m peak-to-peak, with the bipolar spike pointing first along the magnetic field into the ionosphere and then out of the ionosphere. For the observed downward propagation, this corresponds to a positive potential structures (i.e. ion enhancements or electron holes). The speeds were generally >2000 km/s. Although the solitary waves were moving in the same direction as the electron beam, their speeds were much slower, more consistent with the electrons in the core. Large amplitude waves polarized primarily perpendicular to the magnetic field were observed at a frequency of ~140 Hz (near the lower hybrid frequency). Waves of this type are often seen in the plasma sheet boundary crossings (Cattell et al., 1998). The solitary waves often had a repetition rate similar to the frequency of the perpendicular waves.

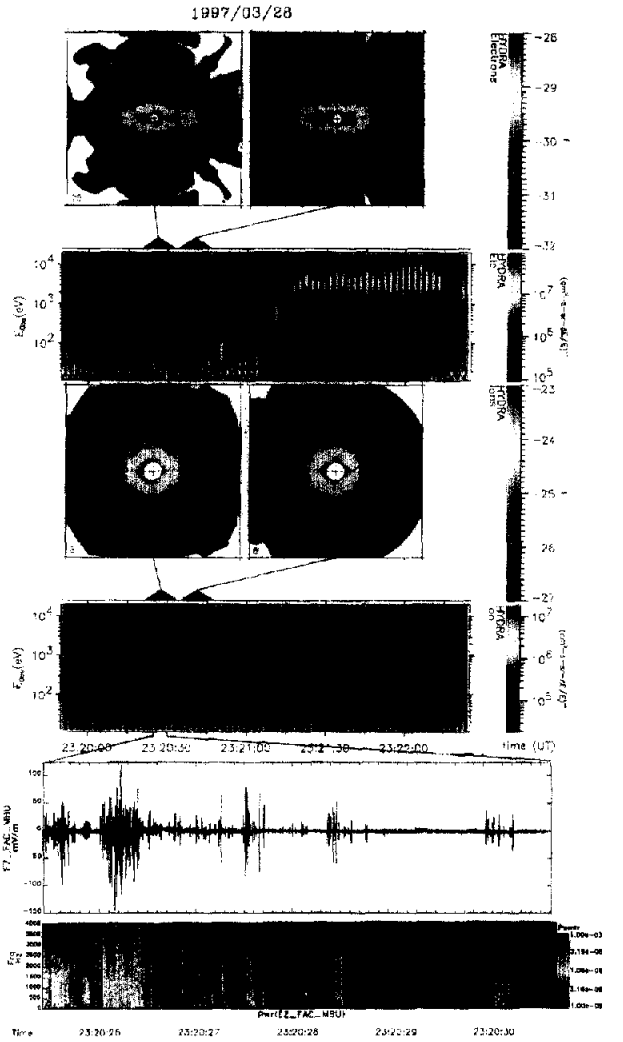

Figure 4. Plasma sheet crossing on March 28, 1997. Same format as Fig. 3.

Figure 4 (same format as Fig. 3 with the addition of a panel containing the Fourier spectrum of the burst data) presents plasma and electric field data from a crossing on March 28, 1997 at an altitude of 6.3 Re and 01:30 MLT. A large-scale view of this plasma sheet boundary crossing is shown in Fig. 2 of Cattell et al. (1999). The waveform burst occurred at a transition between downward and upward current. In the first distribution, there is a strong electron beam moving down the magnetic field peaked at ~10,000 km/s and a less intense beam flowing up the field. In the second distribution, the beams have spread in the parallel direction resulting in a flat-top distribution similar to those observed by FAST at low altitudes. No clear features are observable in the ions. The packets of spiky parallel fields (with broad spectra) are solitary waves. The solitary wave field is first negative (upward) and then positive (downward) with amplitudes up to >50 mV/m. Since the measured time delays correspond to upward velocities (of ~1000 – 2500 km/s), the solitary waves are positive potential structures. In addition, two bursts of Langmuir waves can be seen at ~23:20:29. The

Langmuir wave packets are lower amplitude (~10 mV/m peak-to-peak) than the solitary waves, and occur in a region which is much lower in wave activity than the rest of the burst. Because the duration of this region is less than 1s, it is not possible to determine whether there was a simultaneous change in the electron distribution function.

Very large amplitude solitary waves (up to 200 mV/m peak-to-peak) also occurred at the edge of an intense downward current during a plasma sheet boundary crossing on March 6, 1997, at a radial distance of ~5 Re and 2.5 MLT. The electron distribution on the left, taken at the time of the burst, shows an intense energetic electron beam flowing out of the ionosphere (consistent with the downward current). By the time of the next 12s distribution, the beam direction had changed (consistent with a brief region of upward field-aligned current). Both ion distributions show evidence of perpendicular heating. As was the case in the two previous events, the solitary wave velocity was ~1200->2500 km/s, much slower than the observed electron beam. For the largest solitary waves in this event, large magnetic signatures were observed. Preliminary comparisons to the magnetic field of a moving charge clump, as observed for the FAST electron holes (Ergun et al., 1998), are not consistent with this interpretation.

For all the plasma sheet boundary crossings described above, as well as other cases which have been examined, the solitary waves are positive potential structures, travelling along the magnetic field with velocities of 1000->2500 km/s. The solitary wave velocities are usually in the same direction as simultaneously observed electron beams. The speed is much less than the electron beam, but is consistent with the core electrons. In addition to the bipolar parallel electric field, there are often unipolar perpendicular fields, indicating that the solitary waves are not one-dimensional, as has been observed at low altitudes by FAST (Ergun et al., 1998) and for the small amplitude high altitude events on Polar (Franz et al., 1999). The parallel scale sizes are 10's of λ_D, and, for the largest amplitude structures, $e\Phi/kT_e>\sim1$. Note that there are also many smaller amplitude solitary waves observed in each burst with $e\Phi/kT_e<1$. It should be noted that there were no signatures of the solitary waves observable in the AC magnetic field for most of the events. Only the very largest solitary waves have magnetic signatures.

The question of whether the observed solitary waves could be electron acoustic solitons has been addressed by looking at the regions in parameter space where compressive solitary waves can occur. To obtain compressive solutions, the ions must be hot, i.e. the soliton speed must be less than the ion thermal speed. This is not consistent with the observations which show that the ion thermal speed is always much less than the solitary wave speed. Note that Dubouloz et al. (1999) stated that, for drifting populations, compressive solutions could occur for a large region in parameter space. Muschietti et al. (1999) have shown that electron holes are stable when the ratio of the bounce frequency of electrons in the potential to the electron gyrofrequency was less than 1. For the range of parameters observed for the high altitude solitary waves, this criterion is always met.

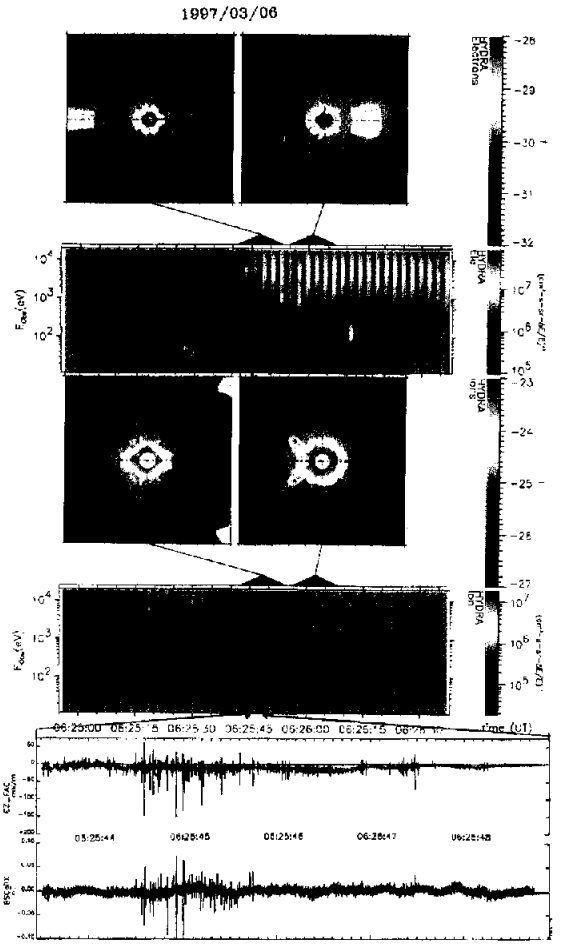

Figure 5. Plasma sheet crossing on March 6, 1997. Same format as Fig. 3.

5 Discussion and conclusions

Previous studies of the electric fields at the plasma sheet boundary, which were restricted to measurements of the component in the ecliptic plane, provided evidence for large amplitude spiky electric fields at radial distances from ~4Re to ~90Re (Mozer, 1981; Cattell et al., 1982; Pedersen et al., 1985; Cattell et al., 1994; Streed et al., 1999). The Polar observations show that, in order to understand the physics of the plasma sheet boundary, it is critical to measure the component of the electric field perpendicular to the ecliptic plane. The Polar instrument has provided the first 3d measurement of the electric field at radial distances up to ~9Re, and, in addition, includes a waveform capture mode with sample rates up to 8000 samples/s. We have reviewed observations made utilizing this capability which show that very large amplitude (up to 100's of mV/m) electric fields are often observed at the plasma sheet boundary on many different time scales from the order of 10^{-3} s to 10^2 s.

Wygant et al. (2000) showed that the longer scales are associated with Alfvenic fluctuations which have their largest electric field normal to the average plane of plasma

sheet (δE_N). The simultaneously observed magnetic field perturbations are azimuthal(δB_T), resulting in a Poynting flux along the geomagnetic field. The observations are consistent with an incompressible, transverse electromagnetic surface shear Alfven mode at the surface of the plasma sheet boundary. The local $\delta E_N/\delta B_T$ is consistent with V_A. The waves provide an intense earthward Poynting flux sufficient to provide the energy necessary for the energization of auroral electron beams. In addition, the intense surface waves are magnetically conjugate (to within 1 degree) to intense auroral emission as determined from the UVI imager, whereas weak aurora are correlated with small amplitude electric fields. Particle detectors simultaneously observe ions flowing up the field line away from the earth, providing further evidence that low altitude acceleration is occurring on conjugate magnetic field lines.

At the shortest scales, solitary waves are ubiquitous and are detected both in regions of downward and upward field-aligned current. In the low altitude auroral zone, both ion modes and electron modes have been distinguished. At high altitudes, however, no ion mode solitary waves have been definitively identified. Polar high altitude observations have shown that solitary waves are often very large amplitude (with parallel electric fields of up to 200 mV/m and $e\Phi/kT_e>\sim1$). The solitary waves are positive potential, fast moving (>~1000 km/s) structures with scale sizes of 10's of Debeye lengths, which are most consistent with an electron hole mode (Cattell et al., 1999). Franz et al. (1998) have described small amplitude solitary waves which have similar characteristics. The low altitude FAST and Polar observations have indicated that the electron hole mode solitary waves are always associated with flat top electron beams, almost always flowing up out of the ionosphere, in a region with $f_{ce}/f_{pe}\sim$ 5-15. Polar and FAST, in addition to previous S3-3 and Viking data, have shown that the ion mode solitary waves are associated with upflowing ion beams and f_{ce}/f_{pe} ~10-50. There are several distinctions between the high altitude solitary waves described herein and the electron holes observed at low altitudes. The high altitude events have no preference for the downward field-aligned current region, while the low altitude ones occur almost exclusively in the downward current region (although they are sometimes observed with very cold beams in upward current regions). There is no clear one-to-one correlation between the types of particle distributions and the solitary waves observed at high altitudes. Although they are often associated with electron beams, the solitary wave velocities are usually much lower than the beam speed. The low altitude events have parallel scale lengths $<\sim2\lambda_D$ in (Ergun et al., 1999), whereas the high altitude events are usually 10's of λ_D. In addition, the electron solitary waves at high altitudes have been observed in regions with fce/ fpe from ~0.1 to >5. Both types of solitary waves at low altitudes are often associated with large amplitude electrostatic ion cyclotron waves which are primarily perpendicular to the geomagnetic field (Temerin et al., 1982 for ion mode solitary waves; Ergun et al., 1999 for electron mode). In the case of high altitude observations, the solitary waves are also often associated with waves which are primarily perpendicular to the geomagnetic field, but the wave frequency is near the lower hybrid frequency, which is much higher than the local ion cyclotron frequency. Note that, in both the low and high altitude cases, these electrostatic waves have frequencies on the order of 100 Hz.

Tests of the amplitude/velocity relationship for the low altitude FAST data (Muschietti et al., 1999) have shown that the low altitude events are consistent with BGK electron holes and not with solitons. Muschietti et al. have also shown that, for the parameter regime usually observed at low altitudes, the holes would be stable. Preliminary studies of compressive electron acoustic solitons suggests that they are unlikely to explain the high altitude solitary waves. This work, combined with the fact that BGK electron holes would be stable for the range of parameters associated with the high altitude solitary waves, suggests that the high altitude events may also be BGK electron holes. The amplitude/velocity relationship for the Polar data is currently being examined to provide a definitive test.

The evolution of electron holes from electron beam instabilities has been addressed by Omura et al. (1996), Matsumoto et al. (1999), Goldman et al. (1999), Mottez et al., (1997) and others referenced therein. These authors have shown that large amplitude solitary waves can result from the evolution of two counterstreaming electron beams. Omura et al. showed that a weak bump on tail resulted in small amplitude solitary waves. Matsumoto et al. (1999) suggested that the small-amplitude solitary waves were due to a weak beam instability when the thermal electrons were hot, whereas Langmuir waves were generated when the thermal electrons were cold. Although the time resolution of the electron distribution measurement is comparable to the length of a waveform capture, we do not find evidence to strongly support these ideas for the generation of the large amplitude solitary waves or the Langmuir waves. We are currently doing simulations based on the observed plasma distributions.

The fact that ion solitary waves have not been observed in the high altitude Polar data may be understood by examining the dependence of the evolution of ion solitons on the background magnetic field. Simulations by Barnes et al. (1985) have suggested that the growth of ion solitary waves requires that the plasma be strongly magnetized ($f_{ce}/f_{pe}>>1$) which is not the case for the observed high altitude events. For the plasma sheet boundary crossings, f_{ce}/f_{pe} is usually on the order of 1; for the cusp cases, $f_{ce}/f_{pe}<1$. Cattell et al. (1999) address the issue of ion solitons at high altitudes in more detail.

Acknowledgments. Analysis of Polar electric and magnetic field data was supported by the NASA International Solar Terrestrial Program under grants NAG 5-3182 and NAG5-3217. Work at the University of Washington was supported by NASA grant NAG 5-3170. Work at the University of Iowa in analysis of

the dependence of the evolution of ion solitons on the background magnetic field. Simulations by Barnes et al. (1985) have suggested that the growth of ion solitary waves requires that the plasma be strongly magnetized ($f_{ce}/f_{pe} >> 1$) which is not the case for the observed high altitude events. For the plasma sheet boundary crossings, f_{ce}/f_{pe} is usually on the order of 1; for the cusp cases, $f_{ce}/f_{pe} < 1$. Cattell et al. (1999) address the issue of ion solitons at high altitudes in more detail.

Acknowledgments. Analysis of Polar electric and magnetic field data was supported by the NASA International Solar Terrestrial Program under grants NAG 5-3182 and NAG5-3217. Work at the University of Washington was supported by NASA grant NAG 5-3170. Work at the University of Iowa in analysis of HYDRA data was performed under NASA grant number NAG 5 2231 and DARA grant 50 OC 8911 0. The results of the HYDRA investigation were made possible by the decade-long hardware efforts of groups led at NASA GSFC by K. Ogilvie, at UNH by R. Torbert, at MPAe by A. Korth and UCSD by W. Fillius. We would also like to thank R. Friedel and co-workers for use of the PAPCO graphical display program and Dr. D. Gurnett for use of the Polar search coil data.

References

Bale, S. et al., Bipolar electrostatic structures in the shock transition region: Evidence of electron phase space holes, *Geophys. Res. Lett.*, **25**, 2929, 1998.

Bostrom, R. et al., Characteristics of solitary waves and double layers in the magnetospheric plasma, *Phys. Rev. Lett.*, **61**, 82, 1988.

Bounds, S. et al., Solitary waves observed by the Polar electric field instrument in the southern hemisphere near 1 Re, *J. Geophys. Res.*, in press, 1999.

Cattell et al., Observations of large amplitude parallel electric field wave packets at the plasma sheet boundary, *Geophys. Res. Lett.*, **25**, 857-900, 1998.

Cattell et al., Comparisons of Polar satellite observations of solitary wave velocities in the plasma sheet boundary and the high altitude cusp to those in the auroral zone, *Geophys. Res. Lett.*, **26**, 425-428. 1999.

Dubouloz, N., et al., Detailed analysis of broadband electrostatic noise in the dayside auroral zone, *J. Geophys. Res.*, **96**, 3565, 1991.

Duboulez, N. et al., IPELS, 1999

Eastman, T.E., L.A. Frank, W.K. Peterson, and W. Lennartsson, The Plasma Sheet Boundary Layer, *J. Geophys. Res*, Vol. 89, No. A3, 1553, 1984.

Ergun, R. et al., FAST satellite observations of large-amplitude solitary wave structures, *Geophys. Res. Lett.*, **25**, 2041-2044, 1998

Ergun, R. et al., Debye-Scale Plasma Structures Associated with Magnetic-Field-Aligned Electric Fields, *Phys. Rev. Lett.*, **81**, 826- 829, 1998.

Franz, J., P. Kintner, and J. Pickett, Polar observations of coherent electric field structures, *Geophys. Res. Lett.*, **25**, 1277-1280, 1998.

Harvey, P. et al., The Electric Field Instrument on the Polar Satellite, in *The Global Geospace Mission*, C.T. Russell, ed., p. 583, 1995.

Goldman, M., M. Oppenheim, and D. Newman, Nonlinear two-stream instabilities as an explanation for auroral biploar wave structures, *Geophys. Res. Lett.*, **26**, 1821-1824, 1999.

Gurnett, D. et al., The Polar Plasma Wave Experiment, in *The Global Geospace Mission*, C.T. Russell, ed., p. 597, 1995.

Hasegawa, A., Particle acceleration by MHD surface wave and formation of the aurora, *J. Geophys. Res.*, 81, 5083, 1976.

Keiling, A. et al., Statistical study of intense electric fields on auroral field lines at 4-7 Re measured with Polar,,submiited to *J. Geophys Res*, 2000

Marchenko, V. and M. K. Hudson, Beam-driven ion acoustic solitary waves in the auroral acceleration region, *J. Geophys. Res.*, **100**, 19791, 1995.

Matsumoto, H. et al., Electrostatic solitary waves (ESW) in the magnetotail: BEN waveforms observed by Geotail, *Geophys. Res. Lett.*, **21**, 2915, 1994.

Matsumoto, H. et al., Generation mechanism of ESW based on th GEOTAIL Plasma Wave Observation, Plasma Observation and Particle Simulation, *Geophys. Res. Lett.*, **26**, 421-424, 1999.

Mottez, F. et al., Coherent structures in the magnetotail triggered by counterstreaming electron beams, *J. Geophys. Res.*, **102**, 11399, 1997.

Mozer, F. S. et al., Micro-physics of the auroral acceleration region and of other regions of the magnetosphere, in*Proc. 21st ESLAB Symp. on Small Scale Plasma Processes*,, Norway, **ESA SP-275**, ed. by B. Battrick, p. 65, European Space Agency, Paris ,1987.

Mozer, F. et al., New features in time domain electric field structures in the auroral acceleration region, *Phys. Rev. Lett.*, **79**, 1281, 1997.

Mushietti, L. et al., Phase-space electron holes along magnetic field lines, *Geophys. Res. Lett.*, **26**, 1093-1096, 1999.

Omura, Y. et al., Electron beam instabilities as the generation mechanism of electrostatic solitary waves in the magnetotail, *J. Geophys. Res*, **101**, 2685, 1996.

Pedersen, A., et al, Electric fields in the plasma sheet and plasma sheet boundary layer, *J. Geophys. Res*, **90**, 1231, 1985.

Pedersen, A., Solar wind and magnetospheric plasma diagnostics by spacecraft electrostatic potential measurements, *Annales Geophysicae, 13*, 118 1995.

Russell, C. T. et al., The GGS/Polar Magnetic Fields Investigation, in *The Global Geospace Mission*, C.T. Russell, ed., p. 563, 1995.

Scudder, J. et al., Hydra- A 3-d electron and ion hot plasma instrument for the Polar spacecraft of the GGS mission, in *The Global Geospace Mission*, C.T. Russell, ed., p. 459, 1995.

Temerin, M. et al., Observations of solitary waves and double layers in the auroral plasma, *Phys. Rev. Lett.*, **48**, 1175, 1982.

Torr M.R., D.G. Torr, M. Zurik, R.B. Johnson, J. Ajello, P. Banks, K. Clark, K. Cole, C. Keffer, G. Parks, B. Tsururanti, and J. Spann, A Far Ultraviolet Imager for the International Solar Terrestrial Physics Mission. in *The Global Geospace Mission*, edited by C.T. Russell, Kluwer Academic Publishers, 1995

Williams, D. J., Energetic ion beams at the edge of the plasmasheet: ISEE observations plus a simple explanatory model, *J. Geophys. Res.*, 86, 5502, 2982

Wygant, J. et al., Polar spacecraft based comparisons of intense electric fields and Poynting flux near and within the tail lobe-plasma sheet boundary to UVI images: An energy source for the aurora *J. Geophys. Res.*, in press (August), 2000.

FIGURES

Figure 1a. Measurements from Polar spacecraft crossing of the PSBL on 5/9/1997. The panels show (from top to bottom) the electron density, the component of electric field approximately normal to the plane of the plasma sheet, the magnetic field (model subtracted) perpendicular to the local magnetic field in the plane of the plasma sheet and the Poynting flux component along the magnetic field. The fourth panel is the total particle energy flux along the magnetic field with positive values corresponding to earthward flux. The fifth panel is the electron density obtained from the Hydra measurements. The two lower two panels display Hydra energy flux-time spectrograms of electrons and ions.

Figure 1b. Hydra electron and ion energy fluxes sorted into pitch angle bins for 5/9/1997.

Figure 2. Images of the aurora from the UVI instrument on the POLAR spacecraft on 5/9/1997. The LBH-long filter used in this image provides an indicator of the total energy deposited in the ionosphere by auroral electrons. The track of the spacecraft is indicated by the small cross (+).

Figure 3. Plasma and electric and magnetic field data for plasma sheet boundary crossing on May 5, 1997. From top to bottom the panels show electron distribution function for two intervals at the burst time, the electron energy time spectrogram, two ion distribution functions, the ion energy-time spectrogram, the east-west component of the magnetic field (indicative of filed-aligned currents), and the field-aligned component of the electric field for the burst.

Figure 4. Plasma sheet crossing on March 28, 1997. Same format as Fig. 3.

Figure 5. Plasma sheet crossing on March 6, 1997. Same format as Fig. 3.